APPLICATION OF DIMENSIONAL ANALYSIS TO RADIATION SHIELDING

by

Walid Constantine Assaf

A Dissertation Submitted to the
Graduate Faculty in Partial Fulfillment of
The Requirements for the Degree of
DOCTOR OF PHILOSOPHY

Major Subject: Nuclear Engineering

Approved:

Signature was redacted for privacy.

In Charge of Major Work

Signature was redacted for privacy.

Head of Major Department

Signature was redacted for privacy.

Dean of Graduate College

Iowa State University
Of Science and Technology
Ames, Iowa

1965

TABLE OF CONTENTS

LIST OF FIGURES

LIST OF TABLES

LIST OF SYMBOLS

$I_o(E)$	incident gamma radiation as a function of energy
$I_\theta(E)$	transmitted gamma radiation as a function of energy
θ	angle which the shield makes with a frontal plane
x	thickness of a shield
λ	a parameter representing any length in general
η	a proposed property of a shielding material
P	the distance from the NaI detector to the shield
Q	oblique thickness of the shield
R	distance from source to shield
μ_m	total mass absorption coefficient
Σ	total macroscopic cross section
ρ	density of the shields
E	characteristic energy of the source
r	counting rate
σ	standard deviation for counting statistics

INTRODUCTION

The methods of dimensional analysis have been useful in many branches of engineering (3,8,11,12). They have provided insight into many complex systems and facilitated the construction of models and prototypes for the purposes of designing hardware, equipment and structures for large engineering operations.

Radiation shielding is, however, an area where engineers have made little or no use of the methods of dimensional analysis. Because of this, the work in this thesis was initiated.

The answers to two basic questions were sought:

1. To what extent is a shield for low-energy gamma radiation a model of one at a higher energy and what are some of the limitations that are involved?
2. Can dimensional analysis be used to extract information concerning a property of the material which is important in radiation shielding design?

In order to arrive at answers to these questions several simple experiments were performed and analyzed. A series of model tests were conducted using lead, concrete, aluminium and iron shields not exceeding a total weight of 300 pounds.

The answers to the questions, as indicated by the results of the analysis and the subsequent experiments and calculations, are encouraging. These seem to indicate that there exists a wealth of applications and experimental techniques in this area if proper efforts are directed toward that end.

REVIEW OF THE LITERATURE

Dimensional Analysis

The literature review is divided into three parts:

A. Introduction

The end result of the method of dimensional analysis is to reduce the number of variables which one must investigate in order to arrive at a solution or a partial solution to any given problem (1).

The ideas underlying the general field of dimensional analysis can be traced to several Greek philosophers (9,10). However, the real development of this field began with Fourier (4) and Rayleigh (13) the latter performed several impressive applications of the method of dimensions.

Two axioms form the basis of dimensional analysis (11):

1. Absolute numerical equality of dimensional quantities may exist only when the two quantities are similar qualitatively.
2. The ratio of the magnitudes of two like quantities is independent of the units used in their measurement, provided that the same units are used for evaluating each.

The axioms and the dimensional methods lend to qualitative relationships among the pertinent variables. An experiment is therefore needed to determine the quantitative relationships if they exist. Nevertheless, the selection of the pertinent variables remains the most important step in the method of dimensional analysis.

B. The Buckingham Pi Theorem

The Buckingham Pi Theorem states that the number of dimensionless and independent groups of variables required to express a relationship

among the pertinent variables in a given phenomenon is equal to the number of variables involved minus the number of dimensions in which those quantities may be measured (11).

Let S = the number of dimensionless and independent groups of variables or pi-terms

N = total number of pertinent variables

B = the number of independent dimensions

Then the Buckingham Pi Theorem states that

$$S = N - B$$

An extension of the above theorem makes possible the design of models and prototypes of engineering systems which are too complex and unyielding for the usual analytical methods of problem solving.

C. Dimensional Analysis and Radiation Shielding

To date little work has been done in this area (5,6,12) although some success was attained by model experiments performed by Mr. Sven A. E. Johansson of the department of Physics at the University of Lund in Sweden (7). Mr. Johansson used an iron shield with an incident gamma-ray energy of 2.62 Mev. for the model experiment. He measured the transmitted gamma-ray strength and after proper normalization compared it to that of the prototype. The prototype shielding experiment consisted of a concrete shield and a gamma-ray source of 7 Mev. The concrete shield was 5.6 times as large as the iron shield. Mr. Johansson found good agreement between model and prototype under certain conditions.

The length of 5.6 to 1 was obtained from the ratios of the densities of the two materials and the Compton cross section at 7 Mev. and 2.62 Mev. In his discussion he reached the conclusion that a model experiment might work at high energies but that it will break down at low energies.

PRELIMINARY ANALYSIS

Several preliminary studies which were designed to show the feasibility of applying dimensional analysis to radiation shielding were performed since work began on this topic late in 1962. The studies produced a variety of ideas which were later dropped on the basis of practical considerations. One prominent idea among these is outlined as follows.

Consider that the following variables are important in the design of a shield:

D = the energy absorbed in the shield per unit of time per unit of volume

C = the curie rating of the source of gamma radiation

E = energy of the gamma radiation per unit of volume of the source

a = thickness of the shield

λ = represents all other lengths

μ = represents some property of the shielding material

The dimensional matrix representing these variables is

	D	C	E	a	λ	μ
F	1	0	1	0	0	1
L	-2	0	-2	1	1	x
T	-1	-1	0	0	0	y

The variables were arranged to form the following pi terms:

$$\frac{D}{CE} = \text{function}\left(\frac{a}{\lambda}, \frac{C^y \mu}{\lambda^{x+2} E}\right) \qquad (1)$$

and a study was carried out to determine whether or not an experiment can

be devised to give information concerning the functional relationship between the terms or shed some light on the nature of μ (the proposed property of the shield) by establishing values for x and y.

Two major problems were encountered. One was the measurement of D, the energy absorbed by the shield and the other was in finding the appropriate types of radioactive sources. Radioactive sources of scaled sizes and energies were required. These had to be intense enough to produce a measurable temperature rise in the shield so that D could be measured. The other alternative consisted of being able tc measure the dose rates due to specific energies of gamma radiation such as the 1.33 Mev. peak from Co-60. These problems widened the scope of the experiments and made the entire project a rather expensive one. Because of this only preliminary experiments were performed before this approach was abandoned.

A simple shielding situation is one created by interposing a material of thickness x between a source and a detector. The shield may be so placed between the source and detector that an angle θ can exist between the vertical side of the shield and the frontal plane, thus the possibility of build-up is not removed even for relatively thin shields. The pertinent variables were assumed to be

$I_o(E)$ = the incident gamma-ray intensity at some specified energy

$I_\theta(E)$ = the transmitted gamma-ray intensity at a specific energy and as a function of the angle which the shield makes with a frontal plane

x = thickness of the material

θ = the angle which the shield makes with a frontal plane

Σ = total macroscopic cross section obtained by multiplying the total mass absorption coefficient (cm^2/gm) by the density of the material

The variables have the following dimensions:

$I_o(E) = T^{-1}$

$I_\theta(E) = T^{-1}$

$x = L$

$\theta = 0$

$\Sigma = L^{-1}$

$I_\theta(E)$ is chosen as the dependent variable therefore one may write:

$$I_\theta(E) = \text{function} \left[I_o(E),\ \theta,\ x,\ \Sigma \right] \tag{2}$$

According to the Buckingham Pi Theorem the existence of five variables and two dimensions implies the existence of three independent pi terms. These are formed by inspection.

$$\frac{I_\theta(E)}{I_o(E)} = f_1(\theta,\ \Sigma x) \tag{3}$$

A similar equation can be written for a second system, the model. Because of this it can be stated that if the two independent pi terms represented by θ and Σx can be held constant for two systems, the transmitted radiation I_θ, after proper normalization, will be identical in both cases. That is, if the following conditions hold

1. $\theta_m = \theta$
2. $(\Sigma x)_m = \Sigma x$

the method of dimensional analysis predicts that relation (4) will

$$\frac{I_\theta(E)}{I_o(E)} = \left[\frac{I_\theta(E)}{I_o(E)} \right]_m \tag{4}$$

hold between two systems, namely those of the model and the prototype. Furthermore, condition (2) above requires that the thickness of the model shield be related to that of the prototype in the following manner:

$$\frac{x_m}{x} = \frac{\Sigma}{\Sigma_m} \tag{5}$$

Relation (5) indicates that the thickness of the model shield and the prototype must form ratios equal to the inverse of the ratios formed by their macroscopic cross section at the appropriate energy intervals.

The predicted ratios which are those of the transmitted to the incident radiation indicated by Equation 4 are interesting. Seemingly these ratios will emerge in normalized form therefore if they are found by experiment no reference will have to be made to the efficiency of the detecting system. This is important since it may be of interest to run the model experiments at a lower characteristic energy and hence gain further flexibility in the testing procedure.

If the performance of the model is the exact duplicate of the prototype, it follows that

$$\frac{\dfrac{I_\theta(E)}{I_o(E)}}{\left[\dfrac{I_\theta(E)}{I_o(E)}\right]_m} = 1.00 \tag{6}$$

Analysis

The application of dimensional analysis is particularly useful in situations where theory is inadequate. In the section on preliminary

analysis, one notes that one of the pi terms depends on a previous knowledge of the mass absorption coefficient and its variation with energy. What is desired is a pi term which contains a quantity capable of describing what the shielding material will do under certain conditions involving multiple scattering. If such a pi term is found for a given material, the testing of models and other shielding systems will be feasible without reference to build-up factors.

With this objective in mind one might examine the dimensions which were involved in Equation 2. Since these were length and time, the assumption will be made that the desired quantity has the dimensions of $L^z T^y$ where z and y are unknown exponents. One of these may be assumed equal to unity.

The pertinent variables in this case are

$I_o(E)$ = the incident gamma-ray intensity at some specified energy range

$I_\theta(E)$ = the transmitted gamma-ray intensity at some specified energy range

x = thickness of the material

λ = represents all other lengths

θ = the angle which the shield makes with a frontal plane

η = property of the material having dimensions $L^z T^y$

The quantity η is chosen as the dependent variable

$$\eta = \text{function}\left[I_\theta(E),\ I_o(E),\ x, \lambda,\ \theta\right] \tag{7}$$

According to the Buckingham Pi Theorem it is noted that there are six

variables and two dimensions, therefore, four dimensionless terms or pi terms are required.

Equation 8 is formed by inspection

$$\left[\eta \frac{I_\theta(E)^y}{x^z}\right] = f_1 \left[\theta, \frac{x}{\lambda}, \frac{I_\theta(E)}{I_o(E)}\right] \tag{8}$$

A similar equation can be written for another system, the model. Because of this, if θ, x/λ and $\frac{I_\theta(E)}{I_o(E)}$ are held constant for the two systems, the quantity to the left of the equality sign in Equation 8 must also be the same for the two systems.

The separability of the terms to the right of the equality sign in Equation 8 is discussed on page 35. The discussion is based on the results of experiments A, B, C, D and E and the conditions for a function to be a "product" and/or a "sum" as discussed by Murphy (11). For the purposes of this particular section the term to the left of the equality sign in Equation 8 was modified by replacing $I_\theta(E)^y$ by $I_o(E)^y$. This simplified the required experiments since $I_o(E)$ represents the incident radiation and only one value of it is needed. If θ, x/λ and $\frac{I_\theta(E)}{I_o(E)}$ combine in a multiplication or additive manner, direct evaluation of η is possible. Restating the similarity conditions required by Equation 8 in mathematical form, we note that if the following conditions are satisfied

1. $\left[\frac{I_\theta(E)}{I_o(E)}\right]_m = \frac{I_\theta(E)}{I_o(E)}$

2. $\theta_m = \theta$

3. $\left[\frac{x}{\lambda}\right]_m = \frac{x}{\lambda}$

then the following relationship must hold

$$\frac{\eta I_\theta(E)^y}{x^z} = \left[\frac{\eta I_\theta(E)^y}{x^z}\right]_m \tag{9}$$

Equation 9 leads to two results (10) and (11) depending on the conditions of the problem.

$$\frac{x}{x_m} = \left[\frac{I_\theta(E)}{I_\theta(E)_m}\right]^{y/z} \tag{10}$$

$$\left[\frac{\eta}{\eta_m}\right] = \frac{I_\theta(E)_m^y \, x^z}{I_\theta(E)^y \, x_m^z} \tag{11}$$

Equation 10 is the result of assuming that the same material will be used in an experiment thus causing η the property of the material to drop out. This form is useful in an experiment where all variables are either known or can be measured therefore enabling one to find values for the exponents y/z. Having values for y/z one can use Equation 11 to find relative values for η for several materials under a specific set up.

The variables x, x_m, $I_\theta(E)$ and $I_\theta(E)_m$ can be measured easily. The thicknesses of the shields are predetermined either by calculating their values or by experimenting with shields of several thicknesses with the objective of meeting the requirement of condition (1) stated on page 9. When this is accomplished, the values for x and x_m become known.

The measurement of the intensity of the incident and of the transmitted gamma radiation is done in the usual manner by using a scintilation detector and a multichannel analyzer. The use of the count rate data will depend on the general purpose of the experiment. One may pick values for the ratio of $I_\theta(E)/I_\theta(E)_m$ from any part of the spectrum in a consistent

manner thus the values of y/z and those for η , the property of the material, will have restricted meaning; the restriction being a function of the materials, the energies of the sources, the energy range at which I_θ is recorded, and the geometry of the experiment.

EXPERIMENTAL PROCEDURE

The experimental set up consisted of a horizontal platform one foot wide by eleven feet long. At one end of the platform a Co-60 or a Cs-137 source was placed facing a scintillation detector using a two-inch NaI crystal (see Fig. 1). The distances between the source and the detector were scaled according to the cross-sections as required by the preliminary analysis, as were the different shields which were placed between the source and the detector.

The intensity, $I_o(E)$, was measured by removing the shield and obtaining a direct count rate from the source. $I_\theta(E)$ was measured by rotating the shield from 0 to 55 degrees whenever possible in 5 or 10 degree intervals and obtaining a count rate of the transmitted radiation. When the Cs-137 source was used the count rate recorded was that of the peak energy 0.662 Mev. For Co-60 the same procedure applied; that is both I_o and I_θ were count rates at a specific energy of 1.33 Mev.

The use of two energies, 0.662 Mev. for the model experiment and 1.33 Mev. for the prototype was intended to show the possibility of reducing the size of the model shield by reducing the energy of the incident radiation. Also it was intended to reduce the effects of multiple scattering and buildup so that hand calculations could be performed either to check the experimental results or augment them.

The scintillation detector was connected to a 400 channel analyzer. The counting times were five minutes live time, for the first six experiments and 2 minutes for experiments A, B, C, D and E. The final count rate which was used in the calculations represented the average of five count rates surrounding the peaks of 0.662 and 1.33 Mev.

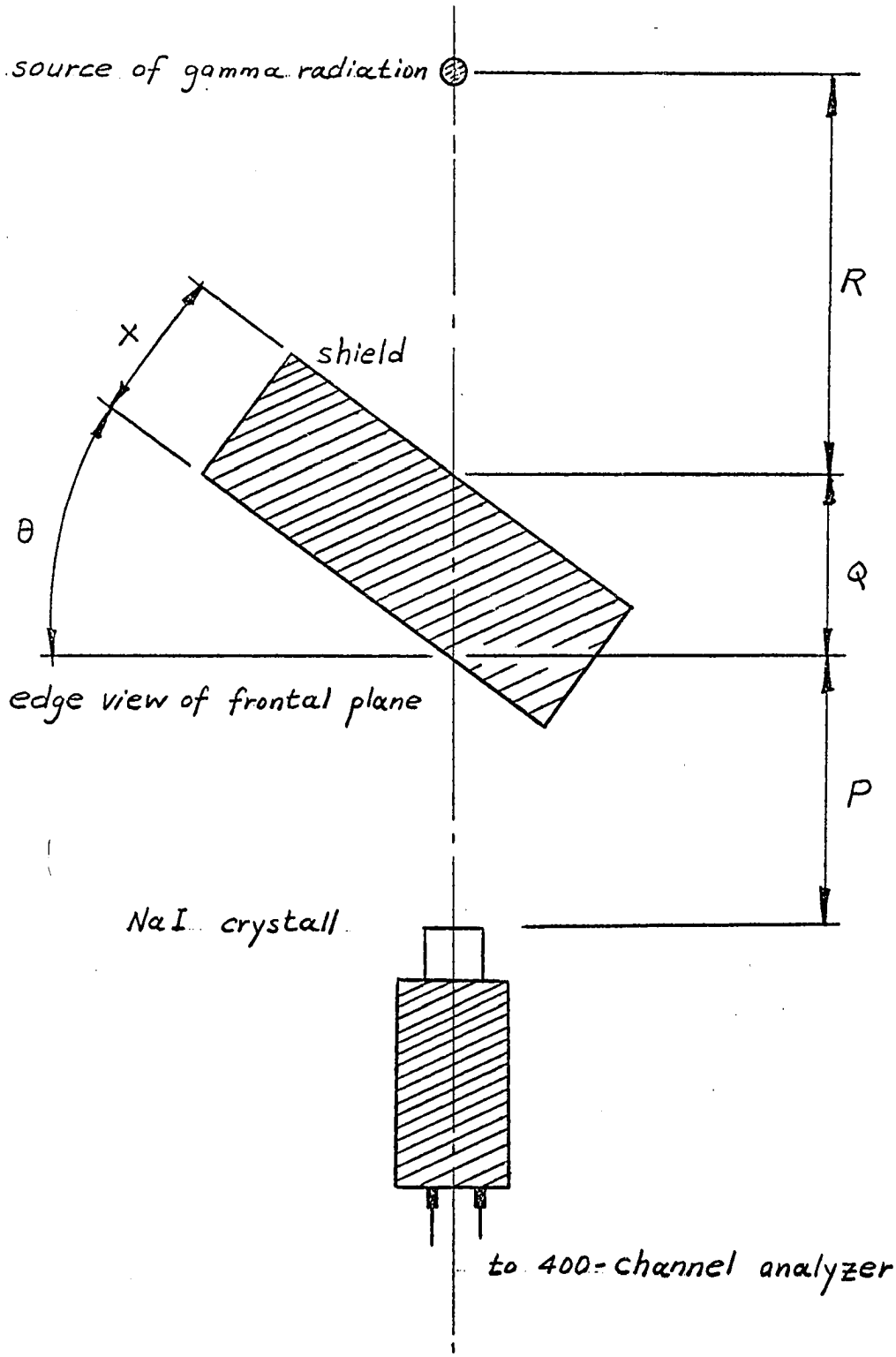

Figure 1. Geometry and basic experimental set-up

Iron, concrete and lead were selected as the shielding materials in the experiments because of their actual utility as shielding materials. Aluminium was used in order to produce data for a low Z material which, unlike concrete, is homogeneous.

Table 1 shows all the materials which were used in the experiments. Their use as model or prototype is indicated as well as the energy of the incident gamma radiation. The total mass absorption coefficient μ_m at 1.33 Mev. and 0.662 Mev. was used to obtain the product ρu_m or Σ and the ratio of this product between the model and the prototype was used as the length scale indicated under x/x_m. All distances and shield sizes were scaled according to this ratio and that includes the distance from source to the shield and shield to the NaI crystal.

The efficiency of the detection system was determined as a function of distance from the source. Fig. 2 shows the results for the two sources which were used throughout this work. The indicated curves were obtained by moving the detector from a distance of 70 inches to within 10 inches of the source and obtaining count rates at convenient positions along the center line between the two. The primary function of this determination was to double check several of the recorded points and also to provide a basis for correction factors in case some distortion in the distances from source to detector became necessary.

The data which were collected from the first six experiments were used for both sections on analysis. However, experiments A, B, C, D and E were performed primarily to determine whether the pi terms to the right of the equality sign in Equation 8 could be separated by addition or multiplication. The appendix shows all the collected data and the calculations which were done to augment the data.

Table 1. List of materials and important properties of the shields used

Expt.	Material	Used As	Energy Mev.	μ_m cm^2/gm	ρ gm/cm^{+3}	Σ cm^{-1}	x/x_m	Required Size Inches
1	Iron	prototype	1.33	0.0510	7.85	0.400	-	2.25 x 5.50 x 8.50
	Concrete	model	0.662	0.0770	2.34	0.180	0.451	5.00 x 12.2 x 18.8
2	Lead	prototype	1.33	0.0540	11.3	0.610	-	1.08 x 2.16 x 4.32
	Concrete	model	0.662	0.0770	2.34	0.180	0.294	3.67 x 7.35 x 14.7
3	Iron	prototype	1.33	0.0510	7.85	0.400	-	2.25 x 5.50 x 8.50
	Iron	model	0.662	0.0740	7.85	0.580	1.47	1.50 x 3.78 x 5.85
4	Lead	prototype	1.33	0.0540	11.3	0.610	-	2.00 x 4.00 x 8.00
	Lead	model	0.662	0.100	11.3	1.13	1.85	1.08 x 2.16 x 4.32
5	Concrete	prototype	1.33	0.0540	2.34	0.126	0	5.70 x 17.1 x 20.0
	Concrete	model	0.662	0.0770	2.34	0.180	1.43	4.00 x 12.0 x 14.0
6	Aluminium	prototype	1.33	0.0520	2.69	0.140	-	3.00 x 7.00 x 7.00
	Aluminium	model	0.662	0.0740	2.69	0.190	1.43	2.10 x 4.90 x 4.90

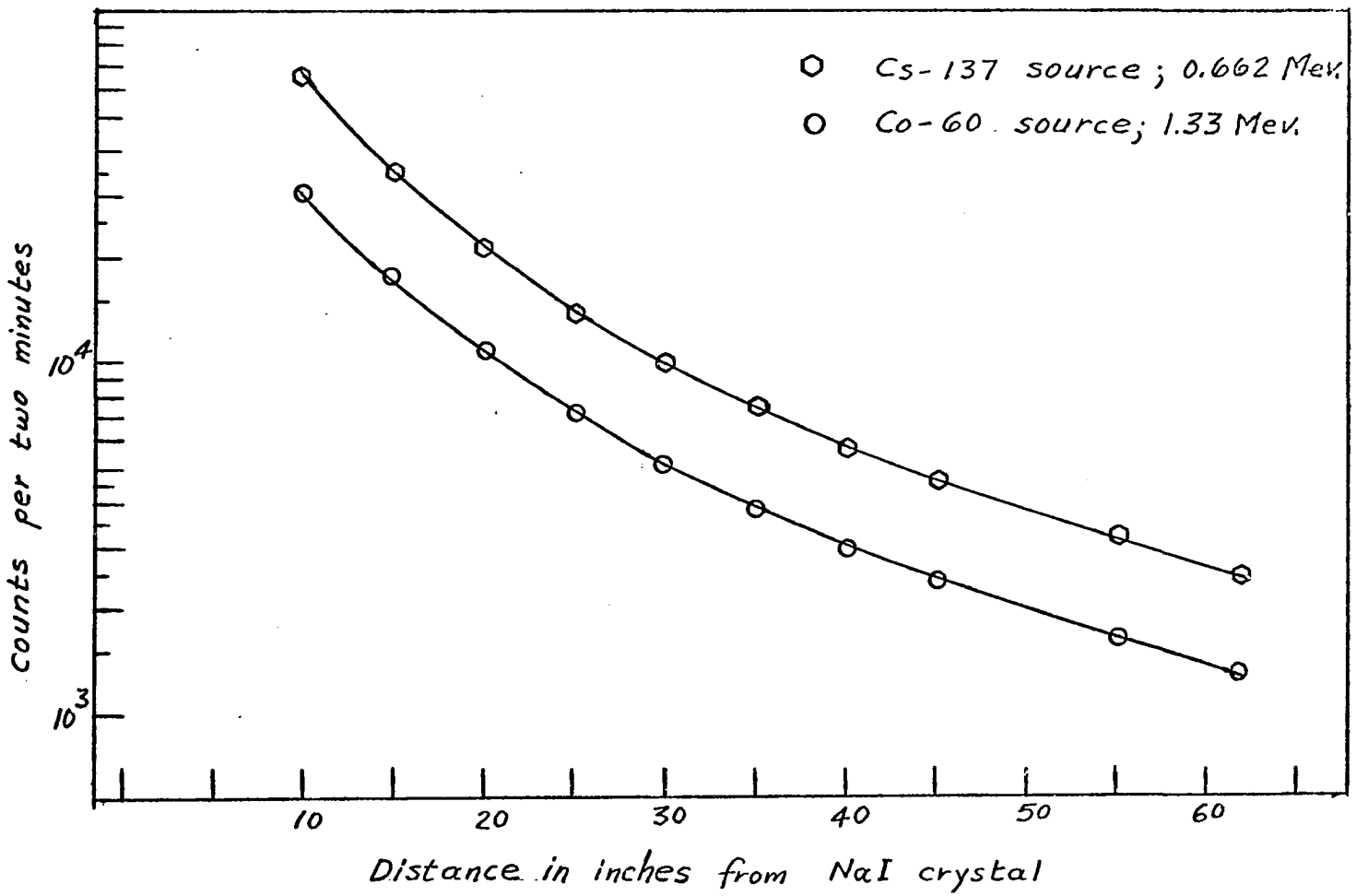

Figure 2. Characteristics of the detecting system

RESULTS

The results of the experiments and the calculations are given in tabular form. Tables 2, 3, 4, 5, 6, 7, 8, 9, 10 and 11 show the results of modeling between several materials in the same order of Table 1. Consider for example Table 2 where an iron shield 2.25 inches thick served as the prototype. Here P represents the distance from the NaI crystal to the shield, Q represents the oblique thickness of the shield and R represents the distance from the shield to the radioactive source, Fig. 1. All distances were measured in inches and to the nearest 1/8 inch. The other quantities which are listed are θ, the angle of the rotation of the shield; I_o, the incident gamma ray count rate; I_θ, the transmitted radiation; x/x_m, the length scale; and the energies, 1.33 Mev. for the prototype and 0.662 Mev. for the model unless specified otherwise. The numbers in the seventh column give the ratios of I_θ/I_o to $\left[I_\theta/I_o\right]_m$ and these should be 1.00 if undistorted modeling is being achieved.

Tables 4, 6, 8 and 10 show all the necessary data needed to solve for the ratio y/z as indicated by Equation 10 on page 10.

Tables 12 and 13 show the results of the calculations using the familiar attenuation equation (see appendix) for calculating relative values for η. Fig. 9 shows the variation in η as a function of energy and the atomic number of the material.

The data of experiments A, B, C, D and E are shown by Tables 18, 19, 20, 21 and 22 in the appendix. Figures 6, 7 and 8 and Tables 14, 15 and 16 show the results of these experiments.

Table 2. Results of iron-concrete experiment

θ	I_o	I_θ	I_θ/I_o	E	x/x_m	$\frac{I_\theta}{I_o} \cdot \left[\frac{I_\theta}{I_o}\right]_m$	P	Q	R	Material
0	23 590	2930	.124	1.33	0.451	-	4.00	2.25	14.0	Iron
5	"	2942	.125	"		-		-		
10	"	2838	.120	"		-		2.29		
15	"	2708	.115	"		-		-		
20	"	2571	.109	"		-		2.43		
25	"	2389	.101	"		-		-		
30	"	2147	.0913	"		-		2.61		
35	"	1870	.0793	"		-		-		
40	"	1600	.0679	"		-		2.94		
45	"	1247	.0528	"		-		-		
50	"	900	.0381	"		-		3.51		
55	"	682	.0289	"		-		-		

Table 2 (Continued)

θ	I_o	I_θ	I_θ/I_o	E	x/x_m	$\frac{I_\theta}{I_o} \div \left[\frac{I_\theta}{I_o}\right]_m$	P	Q	R	Material
0	11 748	1293	.110	.662	0.451	1.13	8.88	5.00	31.0	Concrete
5	"	1303	.111	"		1.13		-		
10	"	1297	.110	"		1.09		5.10		
15	"	1227	.105	"		1.09		-		
20	"	1164	.0994	"		1.09		5.40		
25	"	1085	.0925	"		1.09		-		
30	"	947	.0807	"		1.12		5.80		
35	"	821	.0789	"		1.01		-		
40	"	704	.598	"		1.13		6.50		
45	"	562	.0469	"		1.12		-		
50	"	401	.0351	"		1.08		8.30		
55	"	293	.0250	"		1.15		-		

Table 3. Results of iron-iron experiment

θ	I_o	I_θ	I_θ/I_o	E	x/x_m	$\frac{I_\theta}{I_o} \div \left[\frac{I_\theta}{I_o}\right]_m$	P	Q	R	Material
0	17 796	2195	.123	1.33	1.47	-	9.00	2.25	14.0	Iron
10	"	2165	.122	"		-		2.29		
20	"	1920	.108	"		-		2.43		
30	"	1631	.0917	"		-		2.61		
40	"	1170	.0657	"		-		2.94		
50	"	692	.0389	"		-		3.51		
0	71 584	9239	.128.	.662	1.47	.962	6	1.50	9.35	Iron
10	"	8955	.125	"		.976		1.53		
20	"	8084	.112	"		.960		1.62		
30	"	6705	.0937	"		.977		1.74		
40	"	4966	.0693	"		.949		1.96		
50	"	2976	.0414	"		.964		2.34		

Table 4. Values for y/z resulting from the iron-iron experiment

θ	I_θ/I_o	ln I_θ/I_o	ln x /x_m	y/z	Material
0	.237	-1.44	.400	-.278	Iron
10	.242	-1.42	"	-.282	
20	.238	-1.43	"	-.280	
30	.243	-1.41	"	-.284	
40	.236	-1.44	"	-.278	
50	.233	-1.45	"	-.276	

Table 5. Results of lead-lead experiment

θ	I_o	I_θ	I_θ/I_o	E	x/x_m	$\frac{I_\theta}{I_o} \div \left[\frac{I_\theta}{I_o}\right]_m$	P	Q	P	Material
0	19303	980	.507	1.33	1.85	-	9.27	2.00	12.95	Lead
10	"	929	.481	"		-		2.04		
20	"	798	.413	"		-		2.16		
30	"	637	.0330	"		-		2.32		
40	"	424	.0219	"		-		2.62		
0	130 000	6647	.0510	.662	1.85	.995	5.00	1.08	7.00	Lead
10	"	6405	.0492	"		.979		1.10		
20	"	5580	.0428	"		.965		1.16		
30	"	4413	.0338	"		.975		1.25		
40	"	3083	.0237	"		.925		1.41		

Table 6. Values of y/z resulting from the lead-lead experiment

θ	I_θ/I_o	ln I_θ/I_o	ln x /x_m	y/z	Material
0	.147	-1.92	.615	-.320	Lead
10	.145	-1.93	"	-.318	
20	.143	-1.94	"	-.317	
30	.144	-1.93	"	-.318	
40	.137	-1.98	"	-.310	

Table 7. Results of the concrete-concrete experiment

θ	I_o	I_θ	I_θ/I_o	E	x/x_m	$\frac{I_\theta}{I_o} \div \left[\frac{I_\theta}{I_o}\right]_m$	P	Q	R	Material
0	16 841	3245	.193	1.33	1.43	-	4.00	5.70	14.0	Concrete
10	"	3193	.189	"		-		5.80		
20	"	2908	.172	"		-		6.15		
30	"	2447	.145	"		-		6.60		
40	"	1808	.107	"		-		7.46		
0	69 835	12277	.176	.662	1.43	1.09	2.80	4.00	9.80	Concrete
10	"	12115	.174	"		1.08		4.08		
20	"	11204	.161	"		1.07		4.32		
30	"	9565	.137	"		1.06		4.64		
40	"	7500	.107	"		1.00		5.24		

Table 8. Values of y/z resulting from the concrete-concrete experiment

θ	I_θ/I_o	$\ln I_\theta/I_o$	$\ln x/x_m$	y/z	Material
0	.264	-1.33	.355	-.267	Concrete
10	.263	-1.33	"	-.267	
20	.259	-1.35	"	-.263	
30	.256	-1.36	"	-.260	
40	.240	-1.37	"	-.259	

Table 9. Results of the aluminum-aluminum experiment

θ	I_o	I_θ	I_θ/I_o	E	x/x_m	$\frac{I_\theta}{I_o} \div \left[\frac{I_\theta}{I_o}\right]_m$	P	Q	R	Material
0	12 743	4451	.349	1.33	1.43	-	10.0	3.00	17.0	Aluminium
10	"	4372	.343	"		-		3.06		
20	"	4131	.324	"		-		3.24		
30	"	3806	.299	"		-		3.48		
40	"	3261	.256	"		-		3.93		
50	"	2503	.197	"		-		4.68		
0	52 740	19762	.374	.662	1.43	.932	7.00	2.10	11.9	Aluminium
10	"	19436	.368	"		.933		2.14		
20	"	18763	.354	"		.916		2.27		
30	"	17234	.327	"		.918		2.44		
40	"	15087	.285	"		.899		2.75		
50	"	11824	.224	"		.880		3.28		

Table 10. Values for y/z resulting from the aluminum-aluminum experiment

θ	I_θ/I_o	ln I_θ/I_o	ln x $/x_m$	y/z	Material
0	.226	-1.48	.354	-.239	Aluminium
10	.225	-1.49	"	-.237	
20	.221	-1.50	"	-.236	
30	.222	-1.50	"	-.236	
40	.217	-1.52	"	-.233	
50	.212	-1.55	"	-.228	

Table 11. Results of lead-concrete experiment

θ	I_o	I_θ	I_θ/I_o	E	x/x_m	$\frac{I_\theta}{I_o} \div \left[\frac{I_\theta}{I_o}\right]_m$	P	Q	R	Material
0	55 808	12977	.232	1.33	0.294	-	5.00	1.08	7.00	Lead
10	"	12762	.229	"		-		1.10		
20	"	11999	.215	"		-		1.16		
30	"	10430	.187	"		-		1.25		
40	"	8379	.150	"		-		1.41		
0	11 571	2086	.180	.662	0.294	1.28	17.0	3.67	23.8	Concrete
10	"	2007	.171	"		1.33		3.74		
20	"	1864	.163	"		1.31		3.96		
30	"	1604	.139	"		1.34		4.25		
40	"	1299	.109	"		1.37		4.81		

Table 12. Calculated values for ratios of η

$\frac{\text{(concrete @ 0.66 Mev.)}}{\text{(Al @ 0.66 Mev.)}}$	= 0.883
$\frac{\text{(concrete @ 1.33 Mev.)}}{\text{(Al @ 1.33 Mev.)}}$	= 0.835
$\frac{\text{(concrete @ 1.33 Mev.)}}{\text{(Al @ 0.66 Mev.)}}$	= 1.21
$\frac{\text{(Fe @ 0.66 Mev.)}}{\text{(concrete @ 0.66 Mev.)}}$	= 3.86
$\frac{\text{(Fe @ 1.33 Mev.)}}{\text{(concrete @ 1.33 Mev.)}}$	= 3.63

Table 13. Calculated values for η on the basis that η for aluminium @ 0.662 Mev. is unity

(Concrete @ 0.66 Mev.)	= 0.883
(Al @ 0.66 Mev.)	= 1.00
(Fe @ 0.66 Mev.)	= 3.41
(Concrete @ 1.33 Mev.)	= 1.21
(Al @ 1.33 Mev.)	= 1.45
(Fe @ 1.33 Mev.)	= 4.39

Table 14. Ratios of ordinates from Fig. 6

θ	I_θ/I_o ○	I_θ/I_o △	$\left[I_\theta/I_o\right]_{○} \div \left[I_\theta/I_o\right]_{△}$	Material
0	0.411	0.374	1.10	Aluminium
10	0.400	0.368	1.08	
20	0.384	0.354	1.08	
30	0.356	0.327	1.09	
40	0.312	0.285	1.09	
50	0.250	0.224	1.11	

Table 15. Ratios of ordinates from Fig. 7

x/λ	I_θ/I_o △	I_θ/I_o ⬡	$\left[I_\theta/I_o\right]_{△} \div \left[I_\theta/I_o\right]_{⬡}$	Material
0.10	0.0800	0.0160	5.00	Aluminium
0.12	0.135	0.0300	4.50	
0.14	0.210	0.0500	4.20	
0.16	0.305	0.0760	4.01	

Table 16. Ratio of ordinates from Fig. 8

$I_o x^3$	I_θ/I_o ○	I_θ/I_o △	$\left[I_\theta/I_o\right] \div \left[I_\theta/I_o\right]$ ○ △
0.500×10^6	0.82	0.25	3.3
1.00×10^6	0.22	0.090	2.4
1.50×10^6	0.10	0.050	2.0
2.00×10^6	0.059	0.033	1.8
3.00×10^6	0.027	0.018	1.5

DISCUSSION

As outlined on page 15, six experiments were initially performed for both sections on analysis. These were followed by experiments A, B, C, D and E which were designed to test the separability of the terms in Equation 8. The results of the eleven experiments will be discussed in the above order. The calculations leading to relative values of η are also discussed.

The iron-concrete shielding experiment, Table 2 and Fig. 3, produced essentially the same ratios of I_θ/I_o in both model and prototype. Deviations between the model and the prototype varied from 1% at an angle of 35 degrees to 15% at an angle of 55 degrees. The deviations show no particular trend in this case and are therefore attributed to uncertainties in such terms as the density of concrete and iron and to other deviations such as those resulting from counting statistics (see appendix page 73).

In the next four experiments, lead, iron, concrete and aluminium were used as the shielding materials. The same material was used for both model and prototype per experiment so that values for y/z could be found. The results of these experiments show that the model shields predicted the performance of the prototypes with an error not exceeding 12% (see Tables 3, 5, 7, 9). Because of this, it was possible to find values for y/z as shown in Tables 4, 6, 8, 10. Although these varied from -0.23 to -0.32, it was decided to use the approximate value of -0.3 for the sake of simplicity throughout this thesis.

The results of the concrete-lead experiment, Table 11, show deviations from 28% at an angle of 0 degrees to 37% at an angle of 40 degrees. Because of the differing mechanism of absorption and scattering of gamma

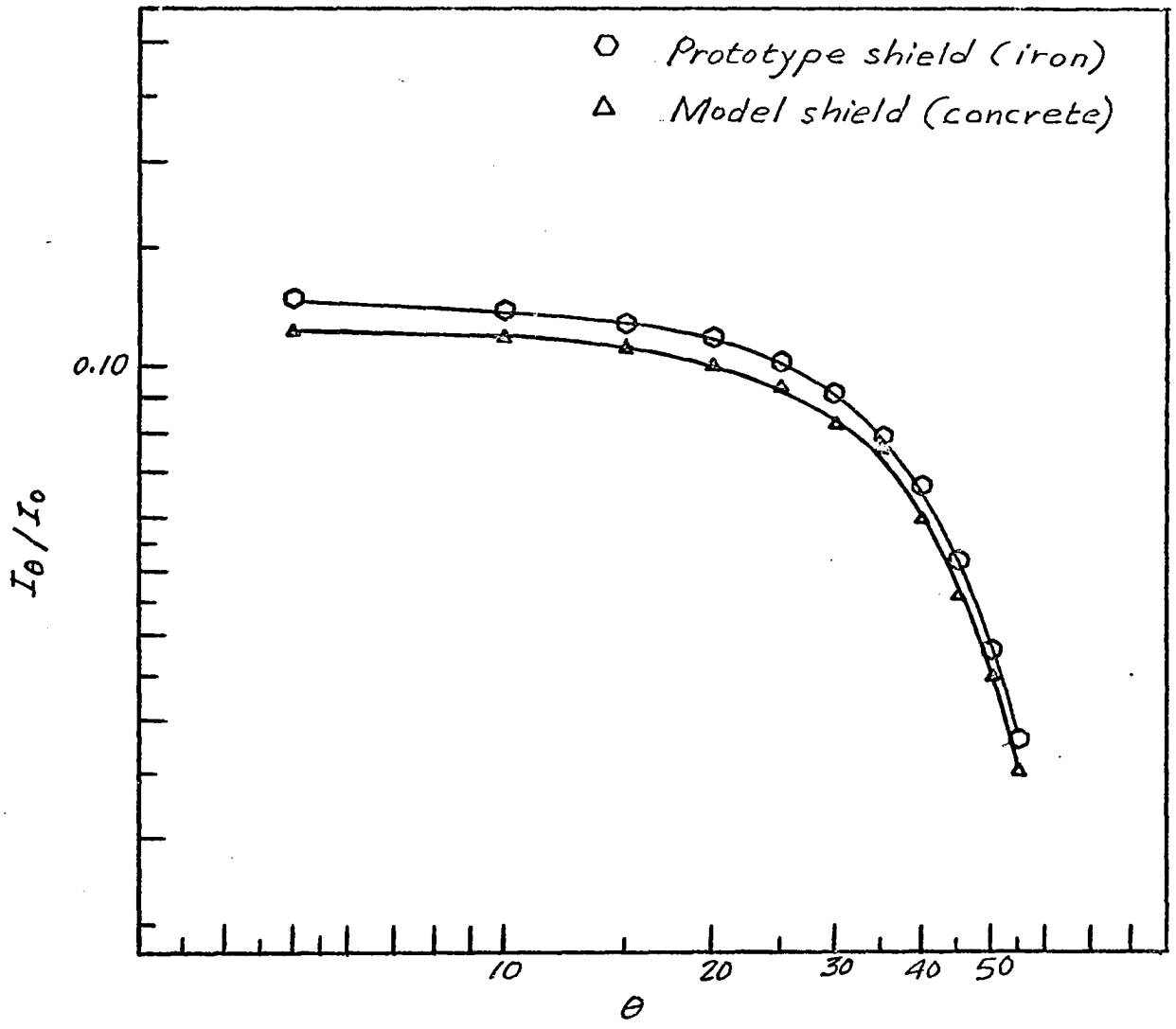

Figure 3. Results of the iron-concrete experiment

radiation in lead and concrete, it was expected that the behavior of the model would differ from that of the prototype (see Fig. 4 and 5).

Experiments A, B, C, D and E were performed using aluminium as the shielding material and the Cs-137 gamma source. Experiment A (Appendix, Table 18) produced values of I_θ/I_o which were compared with those of Table 9 at the same energy of 0.662 Mev. The two curves in Fig. 6 represent two systems each having $\eta I_o^{\ y}\ x^{-z}$ and x/λ held constant while the others varied. The ratios of the ordinates of the two curves are shown in Table 14 for six values of θ. The constancy of this ratio implies that the pi term θ separates from the function f_1 in Equation 8 in a multiplicative fashion (11). That is

$$\frac{\eta\, I_o(E)^y}{x^z} = f_2(\theta)\quad f_3\left[\frac{x}{\lambda}\ ,\ \frac{I_\theta(E)}{I_o(E)}\right] \tag{12}$$

Rewriting Equation 12 to the form shown by Equation 13 and referring to Fig. 6, one determines that the function $f_2(\theta)$ is of the form $e^{-k/\cos\theta}$ where k is a positive constant.

$$\frac{I_\theta(E)}{I_o(E)} = f_2(\theta)\quad f_4\left[\frac{x}{\lambda}\ ,\ \frac{I_o(E)^y}{x^z}\right] \tag{13}$$

The cosine of the angle θ is related to the thickness of the slab, x and to the diagonal distance Q (see Fig. 1) by the equation:

$$\cos\theta = \frac{x}{Q} \tag{14}$$

Therefore Equation 13 takes the familiar form shown by Equation 15, where the function f_4 represents a build-up factor.

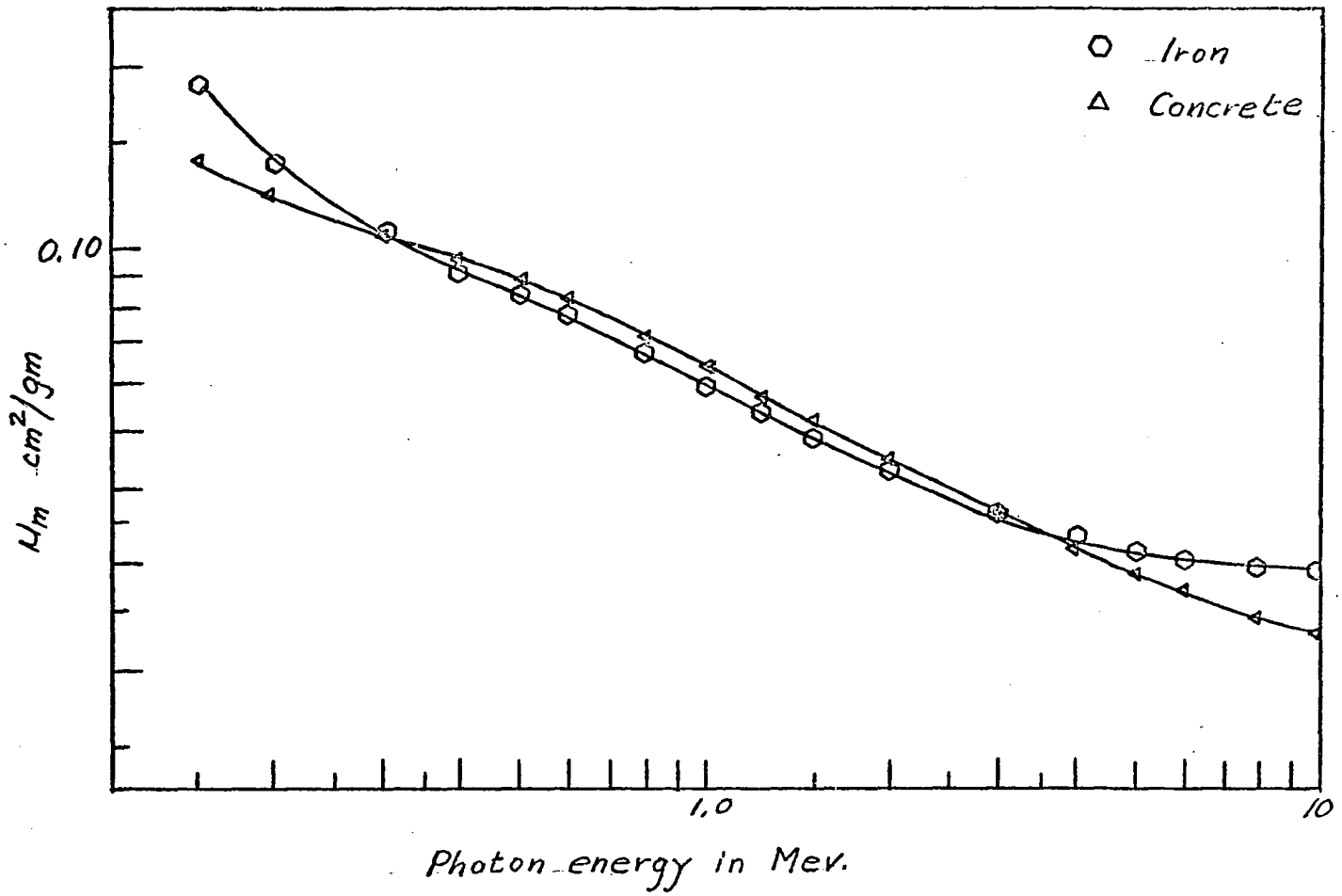

Figure 4. The total mass absorption coefficient, μ_m, as a function of photon energy for iron and concrete

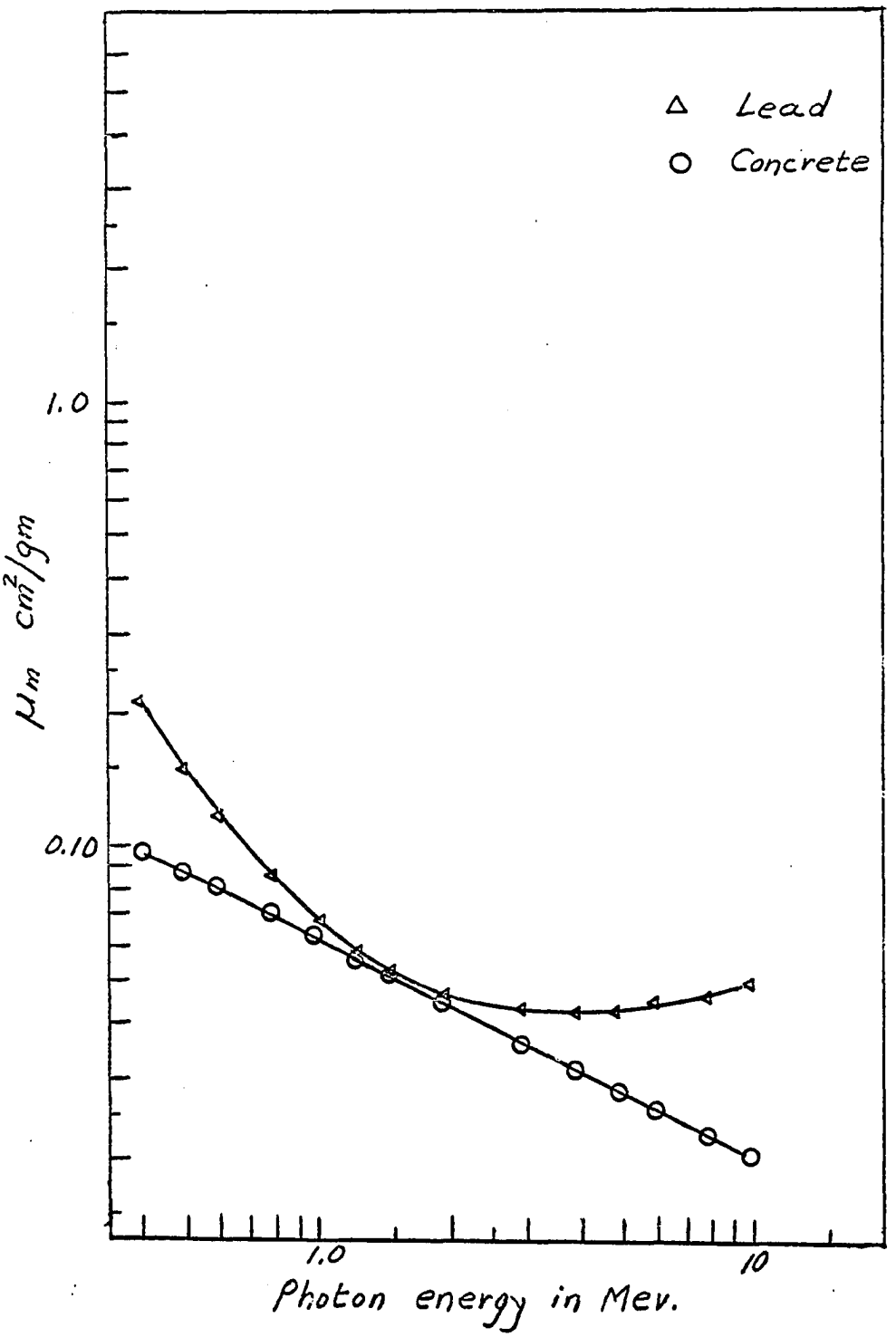

Figure 5. The total mass absorption coefficient μ_m as a function of photon energy for concrete and lead (2)

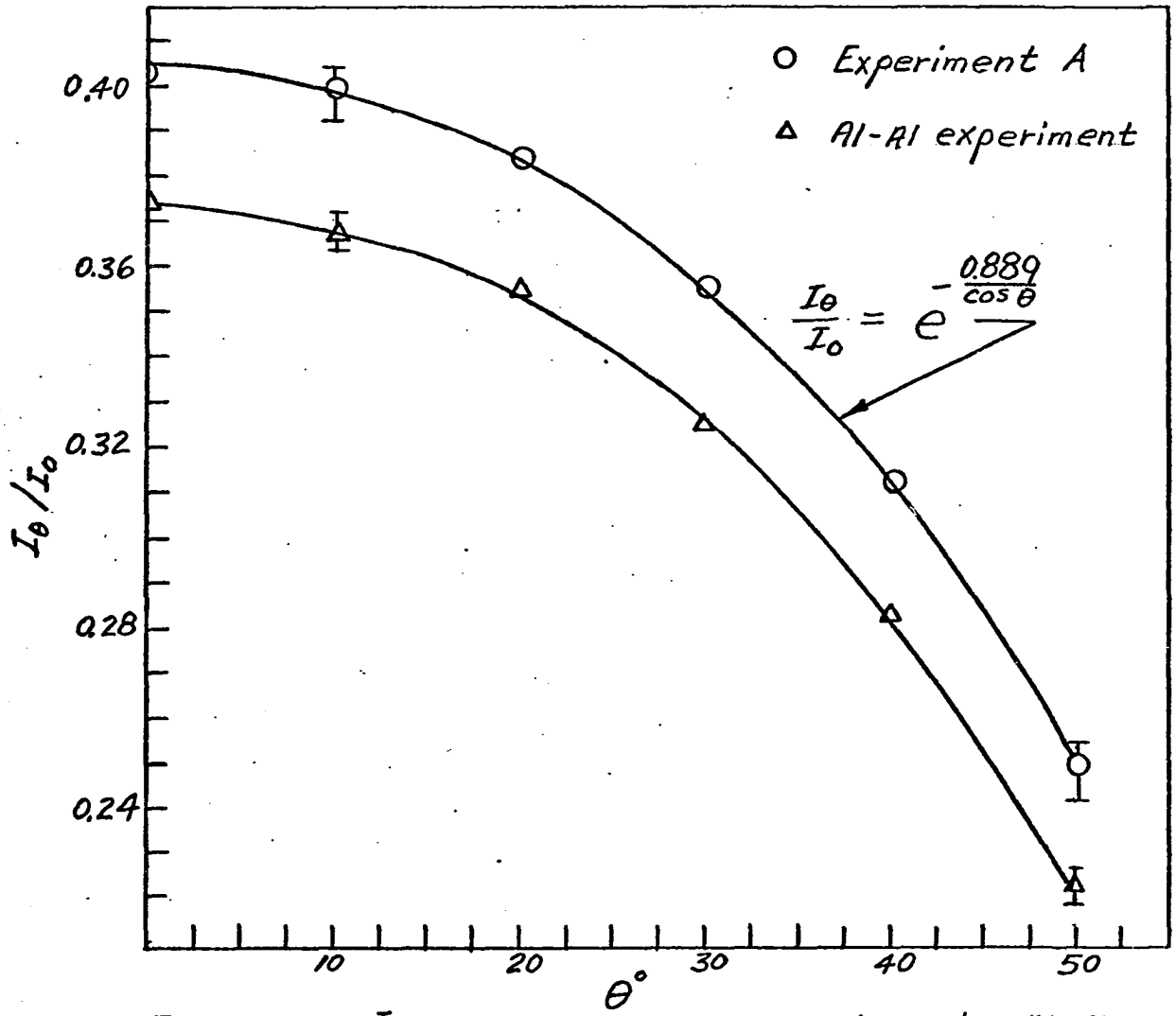

Figure 6. $\frac{I_\theta}{I_o}$ vs. θ for experiment A & the Al-Al experiment

$$\frac{I_\theta(E)}{I_o(E)} = e^{[-k/x]Q} \quad f_4\left[\frac{x}{\lambda}, \frac{\eta I_o(E)^y}{x^z}\right] \tag{15}$$

Experiments B and C (Appendix, Tables 19 and 20) provided data for curves B and C of Fig. 7. Here the terms $\eta I_o(E)^y x^{-z}$ and θ were held constant while I_θ/I_o and x/λ were varied. For these experiments λ was the distance between the source and the detector. The ratio of the ordinates shown in Table 15 show a 25% change over a range of 0.10 to 0.16 for x/λ. Experiments D and E (Appendix, Tables 21 and 22) show the variation of I_θ/I_o as a function of the term $\eta I_o(E)^y x^{-z}$. Since the material was not changed, η was assumed to be unity and using y = 1 and x = -3, the term $\eta I_o(E)^y x^{-z}$ was calculated from experimental values of I_o and x. Table 16 and Fig. 8 show the results of these experiments. The ratio of the ordinates decreased from 3.3 to 1.5 and therefore experiments B, C, D and E show that the terms x/λ and $\eta\frac{I_o(E)^y}{x^z}$ do not separate in a multiplicative manner. Furthermore, since the component sets of data produced by these experiments show slopes other than zero, Fig. 7 and 8, these pi terms can not be combined by addition (11). For this reason a numerical value for η could not be determined. However, ratios of η can be found experimentally for a number of materials. For example, when aluminium is used as a model shield and concrete as the prototype, the ratio of η in concrete to that of aluminium can be found by using Equation 11. In order to find the general trend in the relative values of η as a function of the material's atomic number, one of the needed parameters, I_θ, was approximated by multiplying I_o by the attenuation factor rather than finding it experimentally. Values of I_o were

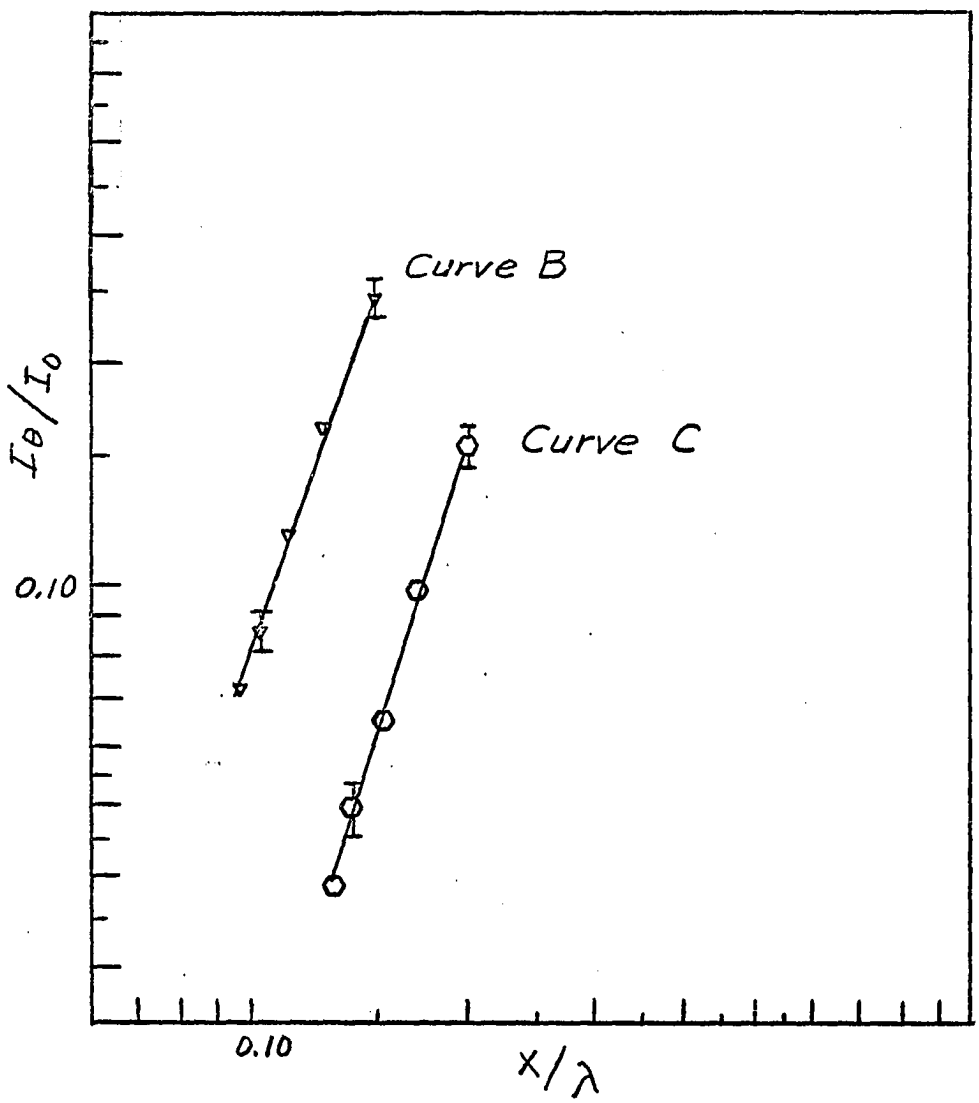

Figure 7. Variation in $\frac{I_\theta}{I_o}$ as a function of $\frac{x}{\lambda}$

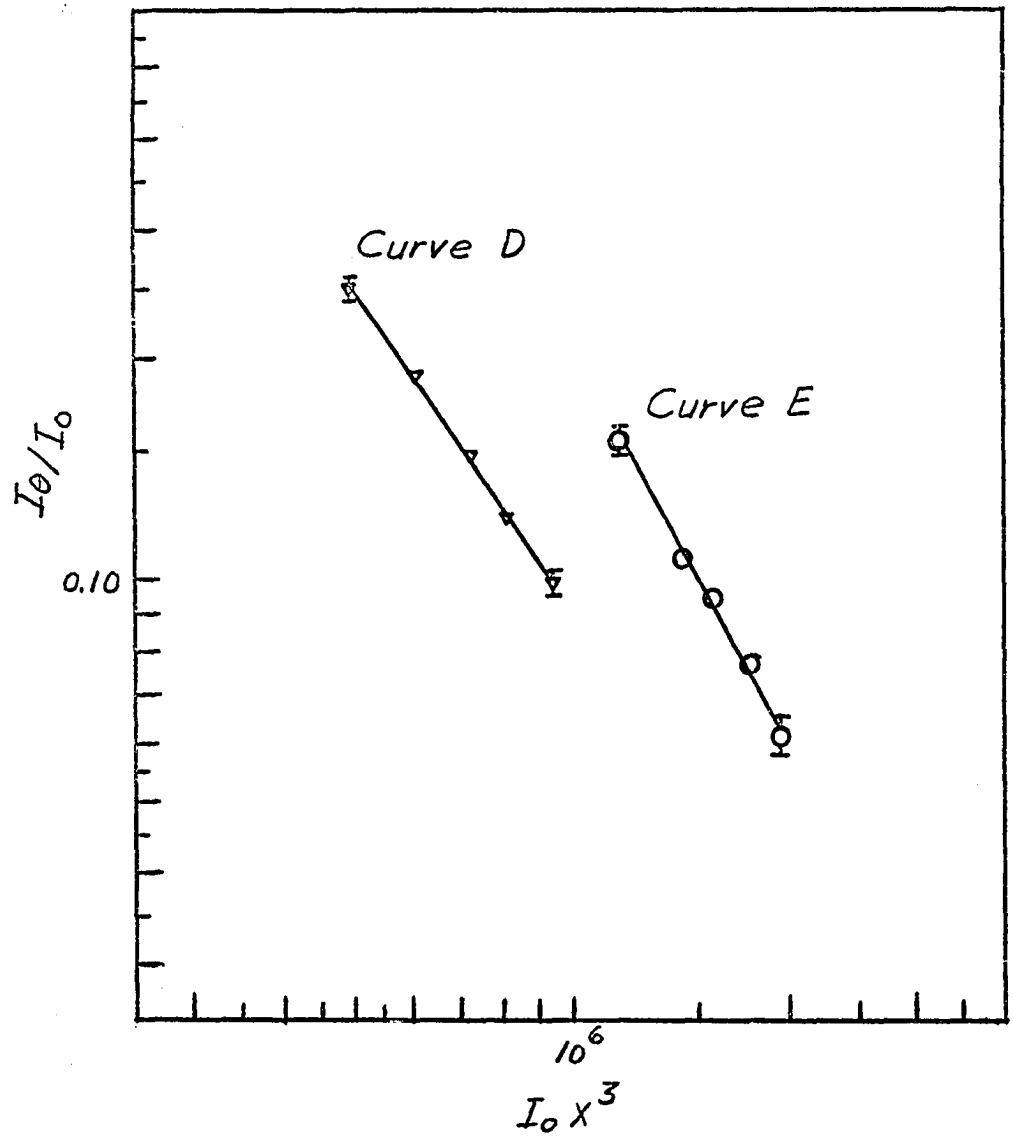

Figure 8. Variation in $\frac{I_\theta}{I_o}$ as a function of $I_o X^3$

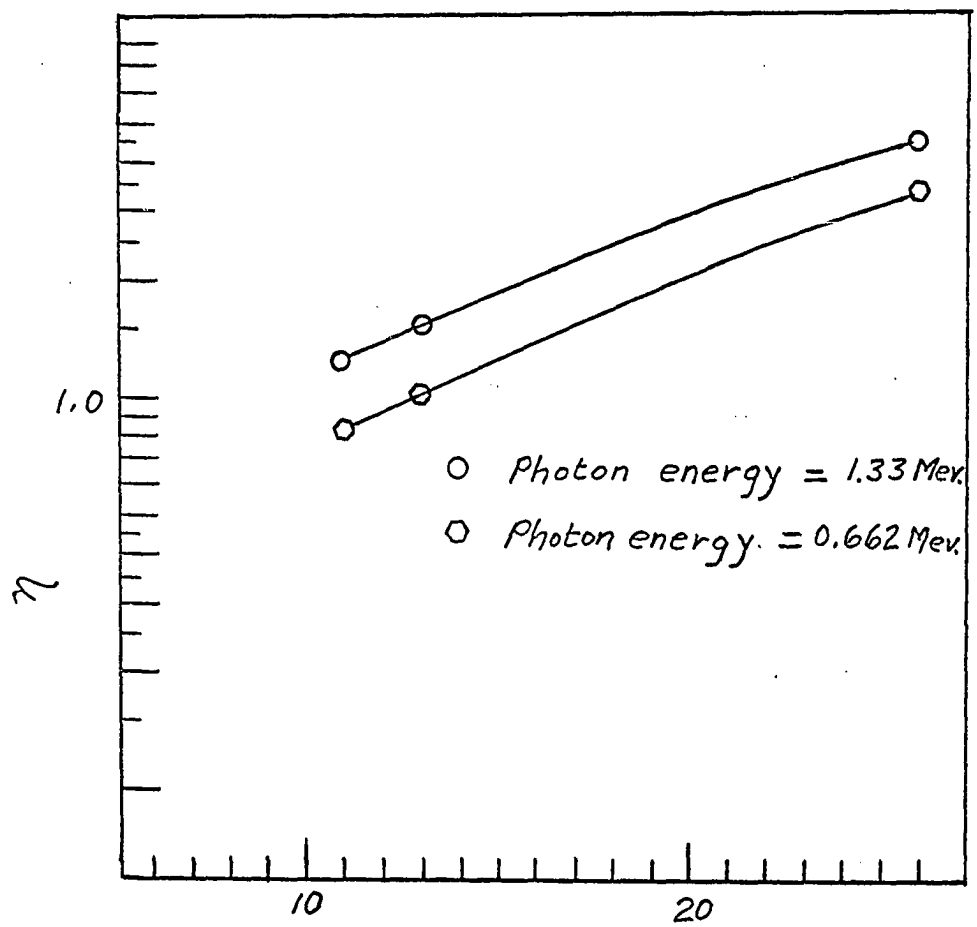

Figure 9. Variation of η as a function of the atomic number of the shielding material (from Table 13)

obtained from the experimental curves of Fig. 2, and as shown in the Appendix (page 71), values for the ratios of η were determined. Variations in the materials and the energy of the incident gamma radiation resulted in five ratios (see Table 12). By assuming that η for aluminium at 0.662 Mev. was unity, six values for η were found and plotted. (see Table 13 and Fig. 9)

Reference to Equation 15 shows the significance of having values for the proposed property of a shielding material and the exponents y/z. According to Equation 15, one can construct a model by requiring the two pi terms, $\frac{\eta I_o(E)^y}{x^z}$ and x/λ to be the same between it and another system, the prototype. Thus the build-up factor represented by the function f_4 becomes the same for both systems and a test of the model shield will yield valuable information concerning the performance of the prototype.

CONCLUSIONS

When build-up factors are not well known for certain geometrical set-ups, as may often be the case, the use of dimensional analysis becomes important. By a series of trials using small models and prototypes, a length scale linking two systems can be found such that I_θ/I_o is the same for both systems. This process fixes other properties of the shield such as density and geometry.

Reference to Equation 15 shows that previous knowledge of parameters such as η , the proposed property of the material, may help in removing build-up variations between model and prototype and thus reduce the problem to simple calculations leading to a knowledge of I_θ/I_o for the prototype shield.

Dimensional Analysis can lead to many empirical equations involving quantities such as η . The development of such relations is possible by supporting the analysis with as much data as is required. Such an endeaver may prove to be a tedious one. Nevertheless, the development of such relations may provide several short cuts in the solution of complex shielding problems.

SUGGESTIONS FOR FURTHER RESEARCH

There are two areas toward which further research may be directed. The first is the recorded data on shielding systems which is present in the literature. One may attempt to extract values for several dimensionless terms for the purpose of forming empirical relations for use in shielding design problems. If this approach is not successful, what changes should be made in the methods of data collection such that the above aim can be realized? The second involves further testing of small models using low level radiation sources. In this area, one may irradiate several small sheets of metal and then combine these to form radioactive sources having different sizes and shapes, such as cubes and cylinders. The effects of the geometrical shape of the source on shield design may then be studied in the light of dimensional analysis. This brings up an important factor and that is the size of the detecting unit. In the case of gamma radiation, one may attempt to find NaI crystals which meet the same length scale requirements as the rest of the system.

BIBLIOGRAPHY

1. Bridgman, P. W. Dimensional analysis. Revised edition. New Haven, Connecticut, Yale University Press. 1931.

2. Etherington, Harold. Nuclear engineering handbook. 1st ed. New York, N.Y., McGraw-Hill Co., Inc. 1958.

3. Focken, C. M. Dimensional methods and their applications. London, England, Edward Arnold and Co. 1953.

4. Fourier, J. B. Theorie analytique de la chaleur. Paris, France, Gauther-Villars et fils. 1822.

5. Goldstein, Herbert. Fundamental aspects of reactor shielding. Reading, Massachusetts, Addison Wesley Publishing Co., Inc. 1959.

6. Heath, Russel La Verne. Scintillation spectrometry. 2nd ed. U. S. Atomic Energy Commission Report IDO-16880-1. [Phillips Petroleum Co. Atomic Energy Division, Idaho Falls, Idaho]. 1964.

7. Johansson, Sven A. E. On the possibility of using model experiments to study shielding problems. Nuclear science and engineering 14, No. 2:96-98. October 1962.

8. Langhaar, Henry L. Dimensional analysis and theory of models. New York, N.Y., John Wiley and Sons, Inc. 1962.

9. Macagno, Enzo D. Historical-critical review of dimensional analysis. Unpublished paper presented at the dimensional analysis, similitude, scaling, and modeling in applied science and engineering meeting, engineering institute, University of Wisconsin, Madison, Wisconsin, March 18-19, 1965. Madison, Wisconsin, Engineering College, University of Wisconsin. 1965.

10. Moody, Ernest Addison. The medieval science of weights. Madison, Wisconsin, University of Wisconsin Press. 1952.

11. Murphy, Glenn. Similitude in engineering. New York, N.Y., The Ronald Press Co. 1950.

12. Ney, Kenneth C. Similitude considerations in neutron and gamma ray scattering. Unpublished M.S. thesis. Ames, Iowa, Library, Iowa State University of Science and Technology. 1955.

13. Rayleigh, John W. S. The principle of similitude. Nature 95:66-68. March 18, 1951.

ACKNOWLEDGMENTS

I wish to express my thanks to Dr. Glenn Murphy for his full support of this investigation and for his many valuable suggestions which made the completion of this thesis possible.

APPENDIX

Table 17. Data for the first six experiments

θ	I_o	channel number	I_θ	channel number	material	used as	E Mev.
0	23 181	252	2808	249	iron	prototype	1.33
	23 987	253	2870	250			
	24 309	254	3085	251			
	23 557	255	2888	252			
	22 919	256	2999	253			
5	"	"	2845	249	"	"	"
			2942	250			
			3043	251			
			2944	252			
			2934	253			
10	"	"	2783	249	"	"	"
			2811	250			
			2902	251			
			2847	252			
			2847	253			
15	"	"	2580	249	"	"	"
			2722	250			
			2833	251			
			2723	252			
			2683	253			

Table 17 (Continued)

θ	I_o	channel number	I_θ	channel number	material	used as	E Mev.
20	"	"	2528	250	"	"	"
			2618	251			
			2624	252			
			2565	253			
			2518	254			
25	"	"	2330	249	iron	prototype	1.33
			2408	250			
			2464	251			
			2364	252			
			2379	253			
30	"	"	2159	250	"	"	"
			2199	251			
			2223	252			
			2154	253			
			2000	254			
35	"	"	1842	250	"	"	"
			1865	251			
			1916	252			
			1908	253			
			1819	254			

Table 17 (Continued)

θ	I_o	channel number	I_θ	channel number	material	used as	E Mev.
40	"	"	1632	250	"	"	"
			1653	251			
			1669	252			
			1619	253			
			1425	254			
45	"	"	1294	250	Iron	protytype	1.33
			1246	251			
			1293	252			
			1193	253			
			1212	254			
50	"	"	828	248	"	"	"
			915	249			
			936	250			
			915	251			
			909	252			
55	"	"	654	249	"	"	"
			685	250			
			727	251			
			698	252			
			648	253			

Table 17 (Continued)

θ	I_o	channel number	I_{θ}	channel number	material	used as	E Mev.
0	11 795	249	1229	244	concrete	model	.662
	11 827	250	1294	245			
	11 922	251	1350	246			
	11 482	252	1280	247			
	11 084	253	1313	248			
5	11 468	248	1242	245	"	"	"
	11 824	249	1323	246			
	11 881	250	1361	247			
	11 863	251	1284	248			
	11 707	252	1306	249			
10	"	"	1274	246	"	"	"
			1307	247			
			1322	248			
			1261	249			
			1322	250			
15	"	"	1188	245	"	"	"
			1167	246			
			1263	247			
			1236	248			
			1280	249			

Table 17 (Continued)

θ	I_o	channel number	I_θ	channel number	material	used as	E Mev.
20	"	"	1165	244	"	"	"
			1155	245			
			1170	246			
			1143	247			
			1189	248			
25	"	"	1081	246	"	"	"
			1115	247			
			1121	248			
			1082	249			
			1026	250			
30	"	"	928	245	"	"	"
			930	246			
			998	247			
			934	248			
			946	249			
35	"	"	775	245	"	"	"
			814	246			
			855	247			
			819	248			
			842	249			

Table 17 (Continued)

θ	I_o	channel number	I_θ	channel number	material	used as	E Mev.
40	"	"	666	244	"	"	"
			715	245			
			712	246			
			697	247			
			729	248			
45	"	"	574	245	"	"	"
			532	246			
			583	247			
			540	248			
			582	249			
50	"	"	405	245	"	"	"
			380	246			
			413	247			
			392	248			
			419	249			
55	"	"	275	245	"	"	"
			300	246			
			303	247			
			301	248			
			289	249			

Table 17 (Continued)

θ	I_o	channel number	I_θ	channel number	material	used as	E Mev.
0	55 821	245	12 689	247	Lead	Prototype	1.33
	56 636	246	13 190	248			
	57 430	247	13 252	249			
	55 564	248	12 842	250			
	53 890	249	12 616	251			
10	"	"	12 203	245	"	"	"
			12 760	246			
			13 101	247			
			12 963	248			
			12 783	249			
20	"	"	11 745	244	"	"	"
			12 136	245			
			12 193	246			
			12 200	247			
			11 725	248			
30	"	"	10 274	244	"	"	"
			10 768	245			
			10 589	246			
			10 463	247			
			10 060	248			

Table 17 (Continued)

θ	I_o	channel number	I_θ	channel number	material	used as	E Mev.
40	"	"	8290	244			
			8428	245			
			8523	246			
			8488	247			
			8166	248			
0	11 478	252	2077	251	concrete	model	.663
	11 721	253	2093	252			
	11 555	254	2102	253			
	11 593	255	2061	254			
	11 509	256	2097	255			
10	"	"	1949	251	"	"	"
			2030	252			
			2045	253			
			1950	254			
			2064	255			
20	"	"	1831	250	"	"	"
			1852	251			
			1911	252			
			1895	253			
			1830	254			

Table 17 (Continued)

θ	I_o	channel number	I_θ	channel number	material	used as	E Mev.
30	"	"	1564	250	"	"	"
			1655	251			
			1699	252			
			1545	253			
			1558	254			
40	"	"	1333	250	"	"	"
			1333	251			
			1290	252			
			1299	253			
			1244	254			
0	17 005	248	2118	242	iron	prototype	1.33
	18 010	249	2129	243			
	18 320	250	2303	245			
	17 974	251	2244	246			
	17 674	252	2182	247			
10	"	"	2184	243	"	"	"
			2165	244			
			2254	245			
			2176	246			
			2055	247			

Table 17 (Continued)

θ	I_o	channel number	I_θ	channel number	material	used as	E Mev.
20	"	"	1935	243	"	"	"
			1983	244			
			1970	245			
			1906	246			
			1806	247			
30	"	"	1599	243	"	"	"
			1622	244			
			1669	245			
			1626	246			
			1641	247			
40	"	"	1144	242	"	"	"
			1188	243			
			1169	244			
			1200	245			
			1149	246			
50	"	"	667	242	"	"	"
			690	243			
			721	244			
			720	245			
			664	246			

Table 17 (Continued)

θ	I_o	channel number	I_θ	channel number	material	used as	E Mev.
0	71 074	246	8794	244	iron	model	.662
	72 758	247	9258	245			
	71 943	248	9427	246			
	71 610	249	9529	247			
	70 535	250	9189	248			
10	"	"	8703	244	"	"	"
			9085	245			
			9004	246			
			9077	247			
			8909	248			
20	"	"	8105	245	"	"	"
			8107	246			
			8227	247			
			8097	248			
			7884	249			
30	"	"	6662	244	"	"	"
			6765	245			
			6851	246			
			6704	247			
			6542	249			

Table 17 (Continued)

θ	I_o	channel number	I_θ	channel number	material	used as	E Mev.
40	"	"	4832	244	"	"	"
			4990	245			
			5047	246			
			5098	247			
			4865	248			
50	"	"	3011	244	"	"	"
			2928	245			
			3046	246			
			2996	247			
			2893	248			
0	19 227	245	940	244	lead	prototype	1.33
	19 450	246	1000	245			
	19 936	247	982	246			
	19 330	248	1025	247			
	18 573	249	954	248			
10	"	"	934	245	"	"	"
			957	246			
			992	247			
			899	248			
			874	249			

Table 17 (Continued)

θ	I_o	channel number	I_θ	channel number	material	used as	E Mev.
20	"	"	813	245	"	"	"
			813	246			
			789	247			
			797	248			
			778	249			
30	"	"	628	244	"	"	"
			640	245			
			664	246			
			628	247			
			625	248			
40	"	"	427	245	"	"	"
			439	246			
			437	247			
			413	248			
			407	249			
0	130 000	250	6545	247	lead	model	.662
			6742	248			
			6823	249			
			6567	250			
			6559	251			

Table 17 (Continued)

θ	I_o	channel number	I_θ	channel number	material	used as	E Mev.
10	"	"	6223	246	"	"	"
			6405	247			
			6545	248			
			6369	249			
			6487	250			
20	"	"	5475	246	"	"	"
			5623	247			
			5581	248			
			5624	249			
			5597	250			
30	"	"	4284	246	"	"	"
			4407	247			
			4437	248			
			4480	249			
			4457	250			
40	"	"	3140	247	"	"	"
			3088	248			
			3138	249			
			3040	250			
			3011	251			

Table 17 (Continued)

θ	I_o	channel number	I_θ	channel number	material	used as	E Mev.
0	16 117	243	3271	244	concrete	prototype	1.33
	16 493	244	3299	245			
	17 260	245	3319	246			
	17 206	246	3258	247			
	17 133	247	3078	248			
10	"	"	3096	243	"	"	"
			3234	244			
			3382	245			
			3235	246			
			3020	247			
20	"	"	2892	244	"	"	"
			2985	245			
			3005	246			
			2879	247			
			2781	248			
30	"	"	2452	244	"	"	"
			2526	245			
			2533	246			
			2439	247			
			2283	248			

Table 17 (Continued)

θ	I_o	channel number	I_θ	channel number	material	used as	E Mev.
40	"	"	1691	242	"	"	"
			1790	243			
			1907	244			
			1874	245			
			1787	246			
0	68 925	250	12 144	245	concrete	model	.662
	70 281	251	12 261	246			
	70 517	252	12 301	247			
	70 530	253	12 357	248			
	68 913	254	12 322	249			
10	"	"	12 110	246	"	"	"
			12 311	247			
			12 077	248			
			12 215	249			
			11 684	250			
20	"	"	11 144	247	"	"	"
			11 418	248			
			11 438	249			
			11 079	250			
			10 942	251			

Table 17 (Continued)

θ	I_o	channel number	I_θ	channel number	material	used as	E Mev.
30	"	"	9421	249	"	"	"
			9556	250			
			9610	251			
			9591	252			
			9648	253			
40	"	"	7411	249	"	"	"
			7578	250			
			7572	251			
			7441	252			
			7500	253			
0	12 543	248	4453	247	Aluminium prototype		1.33
	12 930	249	4462	248			
	12 972	250	4604	249			
	12 814	251	4430	250			
	12 457	252	4305	251			
10	"	"	4458	247	"	"	"
			4373	248			
			4464	249			
			4363	250			
			4201	251			

Table 17 (Continued)

θ	I_o	channel number	I_θ	channel number	material	used as	E Mev.
20	"	"	3982	245	"	"	"
			4071	246			
			4280	247			
			4216	248			
			4106	249			
30	"	"	3754	243	"	"	"
			3752	244			
			3929	245			
			3897	246			
			3699	247			
40	"	"	3242	243	"	"	"
			3320	244			
			3240	245			
			3369	246			
			3136	247			
50	"	"	2458	243	"	"	"
			2548	244			
			2510	245			
			2498	246			
			2504	247			

Table 17 (Continued)

θ	I_o	channel number	I_θ	channel number	material	used as	E Mev.
0	52 740	250	19 742	245	Aluminium	model	.662
			19 696	246			
			20 191	247			
			19 808	248			
			19 375	249			
10	"	"	19 016	249	"	"	"
			19 595	246			
			19 852	247			
			19 513	248			
			19 204	249			
20	"	"	18 572	245	"	"	"
			18 780	246			
			19 039	247			
			18 737	248			
			18 240	249			
30	"	"	17 022	245	"	"	"
			17 394	246			
			17 554	247			
			17 268	248			
			16 931	249			

Table 17 (Continued)

θ	I_o	channel number	I_θ	channel number	material	used as	E Mev.
40	"	"	15 079	245	"	"	"
			15 120	246			
			15 242	247			
			15 212	248			
			14 779	249			
50	"	"	11 547	245	"	"	"
			12 062	246			
			12 003	247			
			11 974	248			
			11 536	249			

Table 18. Data from experiment A

θ	I_o	I_θ	I_θ/I_o	E Mev.	P	Q	R	Material
0	8942	3674	0.411	0.662	7.00	2.00	21.0	Aluminium
10		3579	0.400					
20		3429	0.384					
30		3183	0.356					
40		2792	0.312					
50		2218	0.250					

Table 19. Data from experiment B

θ	x	I_o	I_θ	I_θ/I_o	λ	x/λ	$I_o x^3$
0	3.00	18367	4502	0.245	20.0	0.150	496×10^3
0	3.80	8942	1501	0.168	30.0	0.126	489×10^3
0	4.53	5308	636	0.119	40.0	0.113	493×10^3
0	5.22	3459	304	0.0879	50.0	0.104	492×10^3
0	5.86	2456	175	0.0713	60.0	0.0978	494×10^3

Table 20. Data from experiment C

θ	x	I_o	I_θ	I_θ/I_o	λ	x/λ	$I_o x^3$
0	4.00	18367	2840	0.154	20.0	0.200	1.17×10^6
0	5.08	8942	877	0.0982	30.0	0.169	1.17×10^6
0	6.05	5308	344	0.0647	40.0	0.151	1.17×10^6
0	6.96	3459	171	0.0495	50.0	0.139	1.16×10^6
0	7.80	2456	94	0.0383	60.0	0.130	1.16×10^6

Table 21. Data from experiment D

x	λ	x/λ	θ	$I_o x^3$	I_o	I_θ	I_θ/I_o
3.00	20.0	0.15	0	495×10^3	18367	4574	0.249
3.50	23.3	0.15	0	623×10^3	14500	2765	0.191
4.00	26.6	0.15	0	733×10^3	11450	1697	0.148
4.50	30.0	0.15	0	814×10^3	8942	1066	0.119
5.00	33.3	0.15	0	950×10^3	7600	750	0.0987

Table 22. Data from experiment E

x	λ	x/λ	θ	$I_o x^3$	I_o	I_θ	I_θ/I_o
4.00	20.0	0.20	0	1.17×10^6	18367	2835	0.154
4.50	22.5	0.20	0	1.41×10^6	15500	1805	0.105
5.00	25.0	0.20	0	1.58×10^6	12600	1219	0.0974
5.50	27.5	0.20	0	1.76×10^6	10600	823	0.0776
6.00	30.0	0.20	0	1.93×10^6	8942	537	0.0600

Sample Calculation for Ratios of η:

Materials:

Concrete for the prototype shield
Aluminium for the model shield

Energy of Gamma Radiation:

Prototype: 0.66 Mev.
Model : 0.66 Mev.

Length Scale:

$$\frac{x_m}{x} = \frac{\Sigma \text{ (concrete @ 0.66 Mev.)}}{\Sigma \text{ (Al @ 0.66 Mev.)}} = \frac{(0.0770 \text{ cm}^2\text{gm}^{-1})(2.34 \text{ gm cm}^{-3})}{(0.0740 \text{ cm}^2\text{gm}^{-1})(2.69 \text{ gm cm}^{-3})}$$

$$= 0.903$$

Geometry:

same as Fig. 1
prototype parameters are R = 10.0 Q = 1.00 P = 10.0
model parameters are R = 9.03 Q = 0.903 P = 9.03

Incident and Transmitted Radiation for the Prototype:

I_o for 0.66 Mev. gamma, 21 inches from the NaI crystal is read from Fig. 2

$$I_o = 19{,}900$$

$$I_\theta = 19{,}900\, e^{-\mu x} = 19{,}900\, e^{-(0.0770 \text{cm}^2\text{gm}^{-1})(2.34 \text{gm cm}^{-3})(2.54 \text{cm})}$$

$$= 19{,}900\, e^{-0.457}$$

$$= (19{,}900)(0.633)$$

$$= 12{,}600$$

$$I_\theta/I_o = 0.633$$

Incident and Transmitted Radiation for the Model:

I_o for 0.66 Mev. gamma, 18.9 inches from the NaI crystal is read from Fig. 2

$$I_o = 24{,}000$$

$$I_\theta = 14{,}000\ e^{-ux} = 24{,}000\ e^{-(0.0740)(2.69)(0.903)(2.54)}$$

$$= 24{,}000\ e^{-0.456}$$

$$= (24{,}000)(0.634)$$

$$= 15{,}200$$

$$I_\theta/I_o = 0.634$$

$$I_\theta/I_o \div \left[I_\theta/I_o\right]_m = 1.00$$

Ratio of η/η_m:

$$\frac{\eta}{\eta_m} = \left[\frac{I_{\theta m}}{I_\theta}\right]^y \left[\frac{x}{x_m}\right]^z$$

$$= (15{,}200/12{,}600)^1 (0.903)^{+3}$$

$$= (1.20)(0.740)$$

$$= 0.883$$

Counting Statistics:

The Lowest Counting Rate Recorded:

I_θ = 94 counts in two minutes
(see Appendix, Table 20)

$r = 94 \div 2$

$= 47$

$\sigma = \sqrt{\frac{47}{2}}$

$= 4.8$

$r^{\pm\sigma} = 47 \pm 4.8$

The Highest Counting Rate Recorded:

I_o = 130,000 counts in five minutes
(see Appendix, Page 59)

$r = 130{,}000 \div 5$

$= 26{,}000$

$\sigma = \sqrt{\frac{26{,}000}{5}}$

$= 72$

$r^{\pm\sigma} = 26{,}000^{\pm 72}$